The ESO Slice Project (ESP) galaxy redshift survey[*]

I. Description and first results

G. Vettolani[1], **E. Zucca**[2,1], **G. Zamorani**[2,1], **A. Cappi**[2], **R. Merighi**[2], **M. Mignoli**[2], **G.M. Stirpe**[2], **H. MacGillivray**[3], **C. Collins**[4], **C. Balkowski**[5], **V. Cayatte**[5], **S. Maurogordato**[5], **D. Proust**[5], **G. Chincarini**[6,7], **L. Guzzo**[6], **D. Maccagni**[8], **R. Scaramella**[9], **A. Blanchard**[10], and **M. Ramella**[11]

[1] Istituto di Radioastronomia del CNR, via Gobetti 101, I-40129 Bologna, Italy
[2] Osservatorio Astronomico di Bologna, via Zamboni 33, I-40126 Bologna, Italy
[3] Royal Observatory Edinburgh, Blackford Hill, Edinburgh EH9 3HJ, UK
[4] School of EEEP, Liverpool John-Moores University, Byrom Street, Liverpool L3 3AF, UK
[5] Observatoire de Paris, DAEC, Unité associée au CNRS, D0173 et à l'Université Paris 7, 5 Place J.Janssen, F-92195 Meudon, France
[6] Osservatorio Astronomico di Brera, via Bianchi 46, I-22055 Merate (LC), Italy
[7] Università degli Studi di Milano, via Celoria 16, I-20133 Milano, Italy
[8] Istituto di Fisica Cosmica e Tecnologie Relative, via Bassini 15, I-20133 Milano, Italy
[9] Osservatorio Astronomico di Roma, via Osservatorio 2, I-00040 Monteporzio Catone (RM), Italy
[10] Université L. Pasteur, Observatoire Astronomique, 11 rue de l'Université, F-67000 Strasbourg, France
[11] Osservatorio Astronomico di Trieste, via Tiepolo 11, I-34131 Trieste, Italy

Abstract. The ESO Slice Project (ESP) is a galaxy redshift survey we have recently completed as an ESO Key-Project. The ESP covers 23.3 square degrees in a region close to the South Galactic Pole. The survey is nearly complete (85%) to the limiting magnitude $b_J = 19.4$ and consists of 3342 galaxies with reliable redshift determination.

In this paper, the first in a series that will present the results of the ESP survey, we describe the main characteristics of the survey and briefly discuss the properties of the galaxy sample. From a preliminary spectral analysis of a large sub-sample of 2550 galaxies we find that the fraction of actively star-forming galaxies increases from a few percent for the brightest galaxies up to about 40% for the galaxies fainter than $M = -16.5$ $+5 \log h$.

The most outstanding feature in the ESP redshift distribution is a very significant peak at $z \simeq 0.1$. The detection of similar peaks, at the same distance, in other surveys in the same region of the sky, suggests the presence of a large bidimensional structure perpendicular to the line of sight. The minimum size of this structure would be of the order of 100×50 h^{-1} Mpc, comparable with the size of the Great Wall.

Key words: galaxies: distances and redshifts – luminosity function; cosmology: observations – large-scale structure of the universe

1. Introduction

In the course of the last decade redshift surveys have provided a major advance in our knowledge of the large scale distribution of galaxies and its statistical properties (see for example the review of Giovanelli and Haynes 1991).

Bright, wide angle surveys (e.g. CfA2, Geller and Huchra 1989; SSRS2, da Costa et al. 1994; Perseus-Pisces, Giovanelli and Haynes 1988) cover a large fraction of the sky and provide a clear picture of the nearby universe, up to about 10,000 km/s or 100 h^{-1} Mpc (where $h = H_0/100$). These surveys reveal large structures in the distribution of galaxies: voids of sizes up to 50 h^{-1} Mpc (de Lapparent et al. 1986), and large (> 100 h^{-1} Mpc) bidimensional sheets as for instance the Great Wall within CfA2 (Geller and Huchra 1989), the Southern Wall within SSRS2 (da Costa et al 1994), or the Perseus-Pisces filament (Giovanelli and Haynes 1988).

Strategies alternative to those adopted for the above-mentioned surveys have been used to study the large-scale structure in depth without paying the price of an excessively large increase of the observing time. These strategies include: a) sparse sampling (see Kaiser 1986), as in the Stromlo-APM redshift survey (Loveday et al. 1992); b) chessboard surveys consisting of separated fields covering a large solid angle; c) pencil beam surveys, as in the Broadhurst et al. (1990; BEKS) survey. These deeper surveys have confirmed the texture detected in shallower surveys up to a depth of 40000 - 50000 km/s.

These strategies, while allowing a faster completion of the surveys, sometimes do not allow an unambiguous interpretation
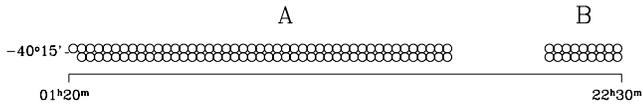
Fig. 1. Survey geometry.

of the data. For example, BEKS report evidence of periodic structures in their first pencil beam redshift survey. However, the real nature of this periodicity is not clear. Moreover, the periodicity is not confirmed in other directions of the sky by the same authors (Koo 1993) and is not detected in other similarly deep redshift surveys even in directions close to the original BEKS pencil beam (Bellanger and de Lapparent 1995).

The present survey (hereafter ESP: ESO Slice Project) was designed to provide an unbiased spectroscopic sample of galaxies brighter than b_J = 19.4, with a high level of completeness, over a region of the sky significantly extended in the right ascension direction. The geometry of the survey, a slice, is the most efficient for mapping three-dimensional structures like those observed in shallower surveys (de Lapparent et al. 1988), provided its thickness is not smaller than the correlation length of the galaxy distribution. Our sample can be used to derive the basic statistical properties of the galaxy distribution, averaged over a volume large enough to smooth out "local" inhomogeneities. With a magnitude limit $b_J \leq$ 19.4 we include L^* galaxies up to $z \simeq 0.16$ and obtain a redshift distribution peaking at $z \simeq 0.1$. Because of the target selection criteria, the ESP is unbiased with respect to a number of statistical descriptors, such as, for example, the luminosity function (see Zucca et al. 1997, Paper II).

The redshift distribution of the ESP galaxies is similar to that of the galaxies in the Las Campanas Redshift Survey (LCRS, Shectman et al. 1996), which covers over 700 square degrees in six strips, each $1.5^o \times 80^o$, and consists of 26418 redshifts of galaxies. The comparison between the two surveys, however, is not straightforward. In fact, ESP galaxies are selected in the photographic blue band, while LCRS galaxies are selected on red CCD frames. Furthermore, contrary to what was done for the LCRS, we did not apply any "a priori" selection on the surface brightness of the target galaxies.

In Sect. 2 we briefly describe the survey region, the galaxy catalogue, the observations and the data reduction; in Sect. 3 we discuss the main spectral properties of the galaxies in our sample; in Sect. 4 we describe qualitatively the large-scale structures detected in our survey. We summarize the main properties of the ESP redshift survey in Sect. 5.

2. General description of the survey

A detailed description of the survey will be presented in the paper containing the whole data catalogue (Vettolani et al. 1997, Paper III, in preparation). Here we briefly summarize the main characteristics of the ESP project.

Table 1. Sample statistics

Sample	Catalogue Objects	Observed Objects	Galaxies with z	Stars	Failed Spectra
strip A	3391	3265	2749	368	147
strip B	1096	779	593	125	61
total	4487	4044	3342	493	208

2.1. The photometric sample

The main area of the ESP survey is a strip 22° long in right ascension and 1° thick in declination (hereafter strip A). In order to make full use of the allotted nights, we were able to survey also an area of $5^o \times 1^o$ (hereafter strip B), five degrees west of strip A. Both strips are located in the region of the South Galactic Pole. The position was chosen in order to minimize the galactic absorption effects ($-60^o \lesssim b^{II} \lesssim -75^o$). The right ascension limits are from 22^h30^m to 22^h52^m for strip B and from 23^h23^m to 01^h20^m for strip A, at the mean declination $\delta = -40^o15'$ (1950).

The target galaxies, with a limiting magnitude b_J = 19.4, were extracted from the Edinburgh-Durham Southern Galaxy Catalogue (EDSGC, Heydon-Dumbleton et al. 1988, 1989), which has been obtained from COSMOS scans of SERC J survey plates. The EDSGC has a 95% completeness at $b_J \leq$ 20.0 and an estimated stellar contamination $\leq 10\%$ (Heydon-Dumbleton et al. 1989).

Preliminary analysis of CCD data, obtained with the 0.9m Dutch/ESO telescope for about 80 galaxies in the magnitude range $16.5 \leq b_J \leq 19.4$ in the region of our survey, shows a linear relation between b_J(EDSGC) and m_B(CCD), with a dispersion (σ_M) of about 0.2 magnitudes around the fit (Garilli et al. in preparation). Since the CCD pointings cover the entire right ascension range of our survey, this σ_M includes both statistical errors within single plates and possible plate-to-plate zero point variations.

We do not have enough information to assess the reliability of magnitudes for the 71 ESP galaxies with $m < 16.5$. It is known that in this bright range various problems may affect the measures, as saturation, ghosts and spikes on plates, the presence of substructure in bright galaxies, or contamination from overlapping bright stars (e.g. Loveday 1996). With this *caveat* in mind, we simply note that presently we do not have evidence for large errors on the magnitudes of bright galaxies in our catalogue, on the basis of a few cases we could check.

2.2. Observations and data reduction

The observations have been obtained during six observing runs (in the period 1991-1993) with the multifiber spectrograph OP-TOPUS (Lund 1986, Avila et al. 1989) at the Cassegrain focus of the ESO 3.6m telescope at La Silla. The geometry of the survey (see Fig. 1) is a regular grid consisting of two rows of adjacent circular fields. Each field has a diameter of 32 arcmin,
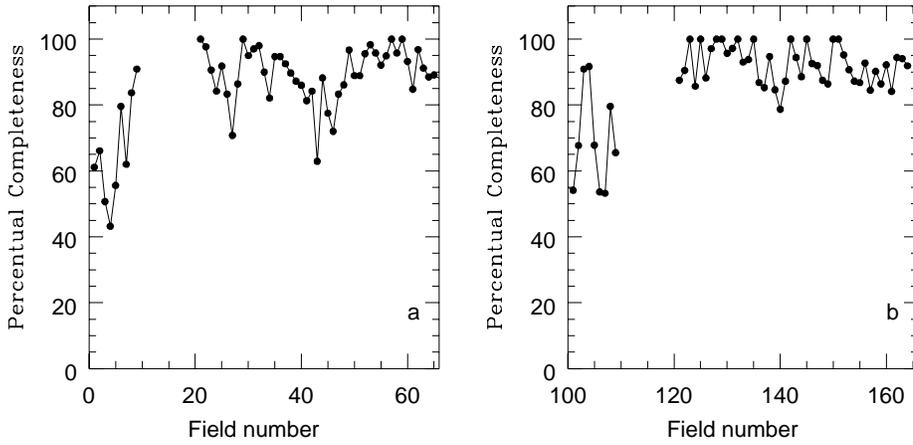
Fig. 2a and b. Redshift completeness for each OPTOPUS field. Field numbers increase with right ascension. **a** Northern row. Field numbers from 1 to 9 correspond to region B; field numbers from 21 to 65 correspond to region A. **b** Southern row. Field numbers from 101 to 109 correspond to region B; field numbers from 121 to 164 correspond to region A.

corresponding to the field of view of the OPTOPUS spectrograph. The two rows of fields are separated by 15 arcmin and slightly overlap each other. The total solid angle is $\sim 7.1 \times 10^{-3}$ steradians (i.e. 23.3 square degrees).

The instrument OPTOPUS has 50 fibers, each with a diameter projected on the sky of $\sim$ 2.5 arcsec. The fibers are manually plugged into holes drilled in aluminum plates at the galaxy positions. For each field we reserved at least 5 fibers for the measurement of the spectrum of the blank sky. On average, there are 35 galaxies brighter than $b_J = 19.4$ per OPTOPUS field and 80% of the fields have fewer than 45 galaxies. When the number of galaxies in a field exceeded the number of available fibers, we selected at random the galaxies to be observed from the total galaxy list. Whenever possible, we re-observed overdense fields in order to reach a higher completeness.

Another set of observations has been obtained in October 1994 with the multifiber MEFOS spectrograph (Felenbok et al. 1997). Thanks to these observations we have been able to observe some of the galaxy spectra that had no redshift determination after the OPTOPUS runs. In particular, we have used these observations to reach a completeness as uniform as possible over all the OPTOPUS fields in strip A.

The spectra cover the wavelength range from 3730Å to 6050Å, with an average pixel size of 4.5Å. We measured the redshifts of the galaxies by cross-correlating the sky-subtracted spectra with a set of 8 template stars. The template stars have been observed with the same instrumental set-up used to obtain the galaxy spectra. We also measured redshifts from the emission lines, whenever present. The median internal velocity error is of the order of $\sim$ 60 km/s. From a comparison of our 8 templates with three SAO radial velocity standard stars we estimate that the zero-point error should be smaller than $\sim$ 10 km/s. We will give a full description of our observations and our reduction procedure in Paper III.

2.3. Sample statistics

We observed a total of 4044 objects, corresponding to $\sim$ 90% of the parent photometric sample of 4487 objects. Out of the 4044 observed objects, 493 turned out to be stars and 208 have a too

low signal-to-noise ratio to provide a reliable redshift (failed spectra). In the end, our final sample consists of a total of 3342 galaxies with reliable redshifts (+ one quasar). About half of the galaxies in our sample have detectable emission lines (see Sect. 3). In Table 1 we report a summary of the basic numbers relative to strip A and strip B.

The mean completeness of our galaxy sample is $\sim$ 85%. We derive this value by assuming that all the failed spectra correspond to galaxies and that the percentage of stars among the 443 objects that were not observed is the same as in the spectroscopic sample (i.e. $\sim$ 12%). The completeness level is significantly different in strip A and in strip B, being 91% for strip A and 64% for strip B. The different completeness level between the two strips is due to our choice of repeating observations only for fields in strip A. Fig. 2 shows the completeness for each OPTOPUS field: panel a) refers to the northern row (field numbers < 100), panel b) to the southern row (field numbers > 100).

A detailed understanding of the completeness and the selection effects is extremely important in any analysis of our data. We therefore performed a number of tests to assess the statistical properties of the galaxies for which we did not measure the spectrum or we did not get a measurable spectrum.

First of all, in the fields where the number of objects is higher than the number of available fibers, the objects we observed are a random subset of the total catalog with respect to both magnitude and surface brightness. The set of observed galaxies departs from randomness only with respect to the selection of the position of the target objects, due to the instrumental constraint that two fibers can not be put closer than about 25 arcsec; obviously this means that when dealing with pairs of galaxies at small projected separation, we could observe only one galaxy (except when the other galaxy was selected for a second exposure).

As far as failed spectra are concerned, we find that the fraction of failed spectra increases at fainter magnitude. However, the fractional increase of failed spectra at fainter magnitudes is not strong, reaching $\sim$ 7% at the limit $b_J = 19.4$. This effect is taken into account in our statistical analysis of the survey (see for example Paper II).

3. The spectral properties of the sample

The ESP data provides a large data-base of galaxy spectra which, when fully analyzed, will constitute a reference for the next generation of larger and deeper redshift surveys that will probe galaxy evolution ($z \geq 0.3$). These data are well suited for the study of the intrinsic properties of galaxies in terms of their stellar populations, and their relation with the environment and redshift (cosmic time). This will be presented in a future paper.

Emission lines are present in a large fraction ($\sim 50\%$) of the galaxies in our sample. We mainly detect [OII] $\lambda3727$, $H\beta$, [OIII] $\lambda4959$ and $\lambda5007$. Our preliminary analysis focused on the [OII] $\lambda3727$ doublet, since this line is the most useful star formation tracer (Kennicutt 1992) in the wavelength range covered by our spectra. Galaxies showing the [OII] $\lambda3727$ line correspond, at increasing equivalent width, to three main categories: spiral galaxies, where the line originates mostly from HII regions in the disks, galaxies undergoing a significant burst of star formation, or AGNs.

Great care is required when dealing with statistical analysis of emission lines properties of galaxies, because the detectability of lines in a spectrum strongly depends on the signal-to-noise ratio S/N of the adjacent continuum. The S/N ratio in the blue part of our spectra ranges from ~ 2 to ~ 10, with an average value of the order of 4. With such a value the [OII] $\lambda3727$ line can be detected only if its equivalent width is larger than about 5 Å. For the spectra of poorer quality, however, the minimum detectable [OII] $\lambda3727$ equivalent width is of the order of 20 Å (see, for example, Fig. 7 in Vettolani et al. 1994). For this reason, in order to properly analyze the distribution of the equivalent widths below 20 Å and to study the possible correlations of the equivalent width with other intrinsic properties, one should also take into account the information carried by the upper limits. In this paper, in order to avoid dealing with upper limits, we present a preliminary analysis of the galaxies with an [OII] $\lambda3727$ equivalent width greater than 20 Å.

Up to now the measurement of the equivalent width of the [OII] $\lambda3727$ line, or of an upper limit for the galaxies in which the line is not detected, has been done for a subsample of 2550 galaxies, corresponding to 76% of the total sample. From this subsample we find that about 13% of the galaxies show an [OII] $\lambda3727$ equivalent width greater than 20 Å and can therefore be classified as actively star-forming galaxies. This fraction, however, is a strong function of absolute magnitude, ranging from a few percent for the brightest galaxies up to about 40% for the galaxies fainter than $M = -16.5 + 5\log h$ (see Fig. 3). This result is qualitatively similar to what has been found in the AUTOFIB Redshift Survey (see Fig. 8 in Ellis et al. 1996). Obviously, this correlation has to be taken into account in the determination of the evolution of the star formation rate as estimated by comparing bright and local samples of galaxies with fainter and more distant ones.
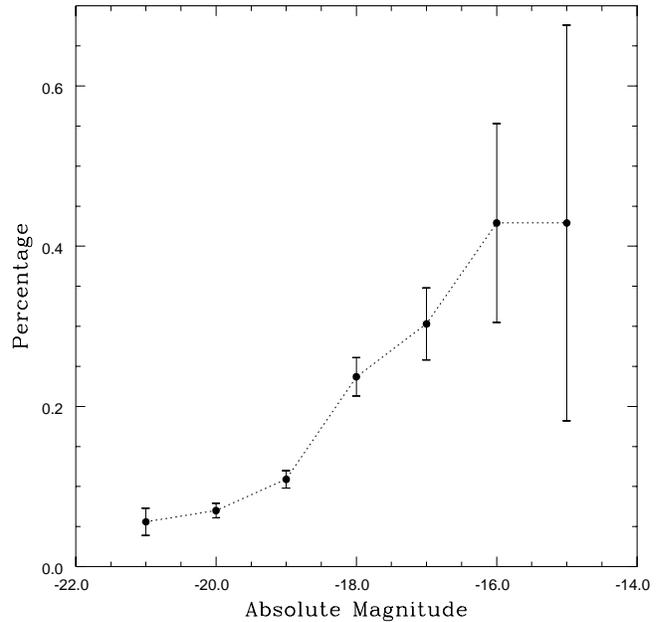

Fig. 3. Percentage of galaxies showing [OII] $\lambda3727$ with an emitted equivalent width greater than 20 Å as a function of absolute magnitude.

4. The large-scale structure

One of the main goals of our survey is to study the properties of the large-scale structure in the local Universe. Our survey is significantly deeper than local surveys (e.g. CfA2 & SSRS2) since M^* galaxies are sampled out to $z \simeq 0.16$, corresponding to a comoving distance $d_{com} \sim 440$ h^{-1} Mpc ($q_0 = 0.5$), which is the effective depth of the sample. This depth, together with a wide extension in the right ascension direction (22° corresponding to ~ 145 h^{-1} Mpc at the effective depth), could be enough to ensure the characteristic of a "fair sample" to ESP. Clearly, the discovery of structures larger than those observed in the existing shallower surveys may prevent even ESP from being a fair sample.

In particular, ESP is deep enough to detect at least the first peaks of the BEKS survey and it is sufficiently wide and thick (~ 6.5 h^{-1} Mpc at $z = 0.16$) to clarify the nature of the peaks that could correspond either to isolated groups/clusters or to the intersection of the beam with a larger connected structure like the Great Wall.

Detailed statistical results, including an analysis of the groups and clusters in the survey, will be presented in forthcoming papers; here we describe the main characteristics of the volume sampled by the ESP.

Fig. 4 shows the histogram of the distribution in comoving distance of the 3342 galaxies with measured redshift (panel a) and the corresponding wedge diagram (panel b). For comparison we show in panel c) the wedge diagram corresponding to the ESP right ascension range from the nearest strip of the LCRS centered at $\delta = -39^o$ (Shectman et al. 1996).

The most outstanding feature in Fig. 4a is the peak at $\simeq$ 290 h^{-1} Mpc . Although about 50 redshifts in this peak are

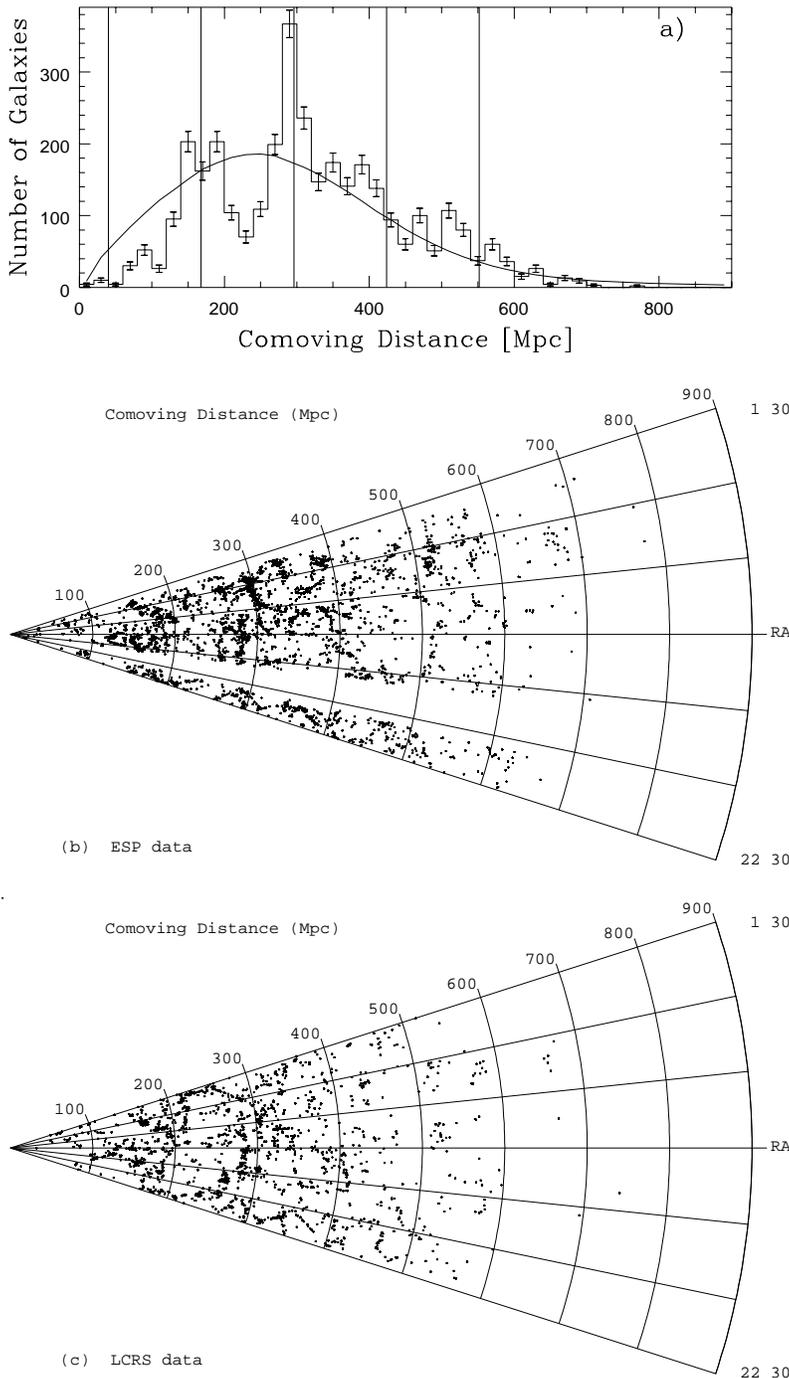**Fig. 4. a** Galaxy distribution in comoving distance ($q_0 = 0.5$); error bars represent 1σ Poissonian uncertainties. The solid line shows the expectation resulting from a uniform distribution of the galaxies in the sample. Vertical lines correspond to the positions of the BEKS peaks (see text). **b** Wedge diagram of ESP galaxies projected in right ascension; the step of the grid is 30^m. **c** The same as panel **b** for galaxies in the LCRS strip centered at $\delta = -39^o$.

due to galaxies within 1 Abell radius from the centers of two Abell clusters (ACO 2840 and ACO 2860) both located near the eastern edge of strip A, this peak remains highly significant even if these galaxies are removed from the sample. In fact, it is clear from Fig. 4b that the peak in the redshift distribution corresponds to an ensemble of large-scale structures nearly perpendicular to the line of sight. If this ensemble can be considered as a single, connected structure, it would have a linear dimension of about 120 h^{-1} Mpc , before entering into the gap between regions A and B. At least part of this structure is visible in the LCRS data (panel c) where it seems to extend towards west and possibly connecting to other structures.

Other foreground/background peaks in the redshift histogram correspond to structures less evident to the eye in the wedge diagram.

Close examination of the wedge diagram shows the existence of many more dense regions and structures, some of which are elongated along the line of sight such as the one in region B stretching from about 130 h^{-1} Mpc to 200 h^{-1} Mpc .

The LCRS data in panel c) allow to follow some of these structures, even if the different sampling, color selection and depth of the samples do not allow a quantitative comparison.

As well as all the other redshift surveys (see for instance panel c), our data suggest the presence of large underdense re-
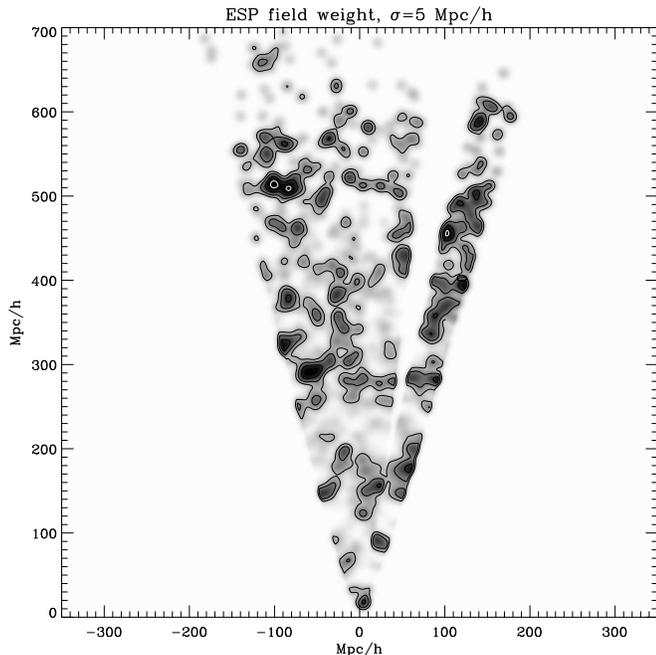
Fig. 5. Smoothed galaxy distribution, obtained by taking into account the survey selection function and the fields incompleteness (see text).

gions. Fig. 4a clearly shows one such region at $d_{com} \simeq 225\ h^{-1}$ Mpc and a second one corresponding to a nearby ($d_{com} \leq 140\ h^{-1}$ Mpc) underdensity.

On the basis of our data and the comparison with the LCRS data, we conclude that this nearby underdense region is statistically significant (see Fig. 4a); however, given the small solid angle covered by ESP and LCRS in this region, it is impossible to assess its extension in the transverse direction. This underdensity has interesting consequences for the interpretation of the bright galaxy counts as we discuss in Paper II.

The vertical lines in Fig. 4a show the location of the regularly spaced density enhancements found in the BEKS pencil beam survey, located at $\alpha = 00^h 54^m$, $\delta = -27.9^o$, i.e. $\sim 12°$ north of the eastern part of the ESP. The two main peaks in our redshift distribution (at comoving distances of ~ 170 and $\sim 290\ h^{-1}$ Mpc) are in reasonably good agreement with the BEKS peaks. The same two peaks are clearly visible in the LCRS data extracted from their slice immediately north ($\delta \sim -39^o$) of our strip. Moreover, the peak at $\sim 290\ h^{-1}$ Mpc appears to be present in the deep pencil beam of Bellanger and de Lapparent (1995), centered at $\alpha = 00^h 19^m$ and $\delta = -30.25^o$, i.e. $\sim 7^o$ away from the BEKS direction. It is also visible in the shallower OPTOPUS probes obtained in this region of the sky by Ettori et al. (1995, see their Fig. 2).

The coincidence in depth of the two nearest peaks of the redshift distribution within ESP with similar peaks in all other surveys in the same region suggests the presence of large extended structures (walls), approximately orthogonal to the line of sight. Under this hypothesis, the structure at $z \simeq 0.1$ would have minimum linear dimensions of the order of $100 \times 50\ h^{-1}$

Mpc , comparable with the size of the Great Wall (Geller and Huchra 1989).

The existence of these two peaks does not imply, however, a periodicity with a preferred scale as claimed by Broadhurst et al. (1990), which can be tested only with much deeper samples.

Fig. 5 shows the density of the *planar projection* of the data. Isodensity contour levels are spaced as 2^j, with $j = 0, 1, ...$: they represent the ratio n_d/n_r of the ESP projected number density n_d, Gaussianly smoothed over 5 h^{-1} Mpc , to the projected number density n_r of a similarly smoothed random field, derived from an average of 100 $3D$ random samples.

Each galaxy was given a weight inversely proportional to the selection function (as derived from the ESP luminosity function, see Paper II), and to the incompleteness of its field. This procedure implicitly assumes that the galaxies we did not observe follow the same distribution in depth as the observed galaxies; this assumption is justified by our random selection of targets in overdense fields. The weighting with the selection function allows to detect structures even at large distances, which would be otherwise "washed out"; however, as any magnitude-limited sample, such structures are inferred from the few high luminosity galaxies that can still be detected, and are therefore affected by a large uncertainty.

The random samples were built using the ESP average luminosity function and K-corrections described in Paper II, and within a three-dimensional space which faithfully takes into account the sample geometry, i.e. not only the unobserved region, but also the presence of a few "holes" in the original catalogue, due to the presence of bright stars.

The final result is a representation of the large-scale galaxy distribution which is more "objective" than the cone-diagram.

In Fig. 5 the dense regions corresponding to the peaks in Fig. 4a are clearly identifiable, in particular the two structures crossing the entire region from one side to the other at comoving distances of ~ 170 and $\sim 290\ h^{-1}$ Mpc . Note also that the most prominent structure at large comoving distance in the small strip B appears to be elongated along the line of sight.

5. Summary

We have presented the main characteristics of the ESO Slice Project, a redshift survey limited to $b_J = 19.4$ in a region near the South Galactic Pole.

This survey, consisting of 3342 galaxies with reliable redshift determination, provides a large data-base of galaxy spectra which will be useful to study the spectral properties of galaxies and will constitute a reference for the next generation of larger and deeper redshift surveys. Preliminary analysis of a large subsample of 2550 galaxies shows a strong anti-correlation between the fraction of galaxies with an [OII] $\lambda 3727$ equivalent width greater than 20 Å and the absolute magnitude. This fraction of actively star-forming galaxies increases from a few percent for the brightest galaxies up to about 40% for the galaxies fainter than $M = -16.5 + 5 \log h$.

Finally, this survey allows the study of the large-scale structure at intermediate depth ($z \sim 0.16$). The most outstanding

feature in the redshift distribution is a very significant peak at $\simeq 290$ h^{-1} Mpc . Similar peaks, at the same distance, are detected in other surveys in the same region of the sky. We conclude that there is evidence for the presence of a large bidimensional structure perpendicular to the line of sight. The minimum size of this structure would be of the order of 100×50 h^{-1} Mpc , comparable with the size of the Great Wall.

References

Avila G., D'Odorico S., Tarenghi M., Guzzo L., 1989, The Messenger 55, 62

Bellanger C., de Lapparent V., 1995, ApJ 455, L103

Broadhurst T.J., Ellis R.S., Koo D.C., Szalay A.S., 1990, Nature 343, 726

da Costa L.N., Geller M.J., Pellegrini P.S., Latham D.W., Fairall A.P., Marzke R.O., Willmer C.N.A., Huchra J.P., Calderon J.H., Ramella M., Kurtz M.J., 1994, ApJ 424, L1

de Lapparent V., Geller M.J., Huchra J.P., 1986, ApJ 302, L1

de Lapparent V., Geller M.J., Huchra J.P., 1988, ApJ 332, 44

Ellis R.S., Colless M., Broadhurst T., Heyl J., Glazebrook K., 1996, MNRAS 280, 235

Ettori S., Guzzo L., Tarenghi M., 1995 MNRAS 276, 689

Felenbok P., Guerin J., Fernandez A., Cayatte V., Balkowski C., Kraan-Korteweg R.C., 1997, Experimental Astronomy, in press

Geller M.J., Huchra J.P., 1989, Science 246, 897

Giovanelli R., Haynes M.P., 1988, in "Large-scale motions in the Universe", Princeton, NJ, Princeton University Press, p.31

Giovanelli R., Haynes M.P., 1991, ARA&A 29, 499

Heydon-Dumbleton N.H., Collins C.A., MacGillivray H.T., 1988, in *Large-Scale Structures in the Universe*, ed. W. Seitter, H.W. Duerbeck and M. Tacke (Springer-Verlag), p. 71

Heydon-Dumbleton N.H., Collins C.A., MacGillivray H.T., 1989, MNRAS 238, 379

Kaiser N., 1986, MNRAS 219, 785

Kennicutt R.C., 1992, ApJ 388, 310

Koo D.C., 1993, in *International Symposium on Observational Cosmology*, G.Chincarini et al. eds., ASP conference series vol.51, p.112

Lin H., Kirshner R.P., Shectman S.A., Landy S.D., Oemler A., Tucker D.L., Schechter P.L., 1996, ApJ 464, 60

Loveday J., 1996, MNRAS 278, 1025

Loveday J., Efstathiou G., Peterson B.A., Maddox S.J., 1992, ApJ 400, L43

Lund G., 1986, OPTOPUS - ESO Operating Manual No. 6, ESO, Garching bei München

Shectman S.A., Landy S.D., Oemler A., Tucker D.L., Lin H., Kirshner R.P., Schechter P.L., 1996, ApJ, 970, 172

Vettolani G. et al., 1994, in *Schloss Ringberg workshop: Studying the Universe with Clusters of Galaxies*, H.Böhringer & S.Schindler eds., MPE report 256, p.7

Vettolani G. et al., 1997, A&A, to be submitted [Paper III]

Zucca E. et al., 1997, A&A, in press [Paper II]